The benefits of age – Improved resistance of mature electroactive biofilm anodes in anaerobic digestion.

*Daniel N. Dzofou [1,2], Falk Harnisch[2], Jörg Kretzschmar[1,]**

[1]DBFZ Deutsches Biomasseforschungszentrum gemeinnützige GmbH (German Biomass Research Centre), Biochemical Conversion Department, Torgauer Straße 116, 04347 Leipzig

[2]Helmholtz Centre for Environmental Research - UFZ, Department of Environmental Microbiology, Leipzig, Germany

KEYWORDS: bioelectrochemical systems, methanogens, alternative electron acceptors, direct interspecies electron transfer,

ABSTRACT

Anaerobic digestion (AD) and microbial electrochemical technologies (MET) can be combined in manifold ways. Recent studies show negative influences of AD effluents on the performance of pre-grown *Geobacter* spp. dominated biofilm anodes. In this study, it was investigated how such biofilm anodes are affected by AD effluents. Therefore, experiments using AD effluent in different concentrations (0% - 100%) at biofilms of different age were performed. Furthermore, the activity of methanogens was inhibited and minimized by application of 2-Bromoethanesulfonate (2-BES)

and microfiltration, respectively. Biofilms pre-grown for 5 weeks show higher resistance against AD effluents compared to biofilms pre-grown for only 3 weeks. Nevertheless, adaptation of biofilms to AD effluents was not successful. Biofilm activity in terms of CE and j_{max} dropped by factor 32.2 ± 3.2 and 38.9 ± 8.4, respectively. The application of 2-BES as well as microfiltration had positive effects on the biofilm activity. The results support the assumption that methanogens or further compounds not studied here, e.g., protozoans, which may have been inhibited or removed by 2-BES application or microfiltration, have an immediate influence on the stability of *Geobacter* spp. dominated biofilms and may limit their practical application in AD environments.

GRAPHICAL ABSTRACT

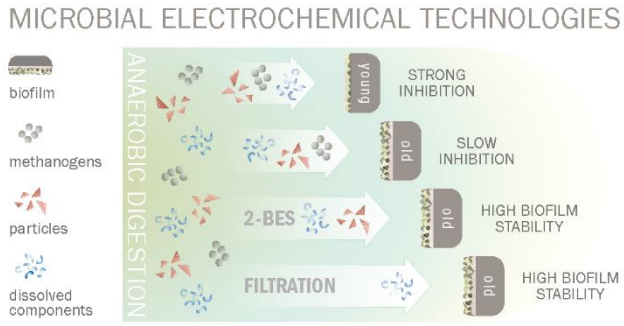

Introduction

Anaerobic digestion (AD) is a common and well established environmental biotechnology for wastewater and sludge treatment or transformation of organic waste into biogas. In AD organic residues, e.g., organic household waste, manure and agricultural residues are broken down in a four-stage microbiological process (including hydrolysis, acidogenesis, acetogenesis and methanogenesis) and are converted to a mixture of carbon dioxide (CO_2) and methane (CH_4)[1,2].

This mixture can, due to the high caloric value of CH_4, be used to produce electrical power and heat or be upgraded by CO_2 removal to CH_4 being injected into the gas grid[1].

In contrast to the well-established AD, microbial electrochemical technologies (MET) are a much younger and less developed environmental biotechnology[3]. MET are defined as technologies or applications that utilize the electrochemical interaction of microorganisms and electrodes[3–5]. This includes oxidative (anodic oxidation) as well as reductive (cathodic reduction) processes where electroactive microorganisms (EAM) act as biocatalyst. For example the oxidation of volatile fatty acids (VFA) to carbon dioxide, electrons and protons at the anode or reduction of CO_2 to CH_4 and water at the cathode[6–8]. MET are discussed to be used in anaerobic wastewater treatment[4,9–11], soil remediation[12], AD process monitoring[13], or the production of methane[3] and hydrogen[13–19], amongst others. The use of, e.g., microbial fuel cells (MFC) for anaerobic wastewater treatment provides advantages over aerobic wastewater treatment in terms of energy and sludge reduction when compared to aerobic treatment [13].

Due to similar fields of application, substrates (e.g. wastewater) or process conditions (e.g. neutral pH, mesophilic temperature, high salinity), AD and MET can be combined in manifold ways: 1) to remove monovalent ions such as ammonium from AD[20], 2) to polish the effluent from AD reactors in terms of COD removal[21], 3) to increase the CH_4 concentration in biogas[22] or 4) to monitor AD with microbial electrochemical sensors[23]. However, recent studies showed also negative influences of AD effluents on the performance of anodic electroactive biofilms[23]. In this specific example, the performance (current density, *j*), of pre-grown *Geobacter* spp. dominated biofilm anodes, i.e., biofilms of *Geobacter* spp. embedded in its self-produced matrix of exopolymeric substances (EPS) on an electrode, decreased within 8 days after integration in a lab scale AD reactor. Visual examination of the biofilms after removal from the AD reactor indicated

57 disintegration of the biofilm morphology. Decreased current density is also observed in anodic
58 chambers of MFC where AD occurs. Very often, this behavior is discussed as substrate
59 competition between methanogens and electroactive bacteria, e.g., reported by Tartakovsky *et*
60 *al.*[24].

61 In AD, manifold different microorganisms as well as dissolved chemical compounds and solids
62 are present that can interfere with EAM. Interference can range from substrate competition with
63 methanogens, e.g., for acetate, over the use of available terminal electron acceptors (TEA) others
64 than the anode, to toxicity of specific compounds, as shown, e.g., for ammonium[25]. Using TEA
65 others than the anode enables survival of EAM outside of biofilms, likely with fewer constraints
66 in terms of substrate availability or mass transfer[23,26,27]. Alternative TEA that occur in AD are
67 manifold, including for instance humic substances, iron and sulphur minerals or even other
68 microorganisms like methanogenic archaea that enable direct interspecies electron transfer
69 (DIET)[28–33]. Using DIET, some methanogenic archaea, e.g., *Methanosarcina barkeri,* or *M.*
70 *horonobensis*[34]*,* are able to accept electrons directly from *Geobacter* spp. to produce CH_4. DIET
71 does not only improve the diversity of electron acceptors, it also introduces new syntrophic
72 interactions between bacteria and archaea, in complex environments that may improve the stability
73 of the microbial community[7,35–37].

74 Interaction of electroactive microorganism in biofilm anodes with compounds or
75 microorganisms within the AD process are so far not well understood, whereas the advantages of
76 AD and MET combinations are evident. Therefore, deeper understanding of these interactions is
77 of great interest to increase the stability of electroactive biofilms in AD environments.

78 In the present study we show that beside substrate competition also structural degradation of
79 *Geobacter* spp. dominated biofilm anodes can occur under AD conditions and that this behavior

80 is most probably induced by methanogens. Consequently, we investigate if and how effluents from
81 AD reactors affect the stability of *Geobacter* spp. dominated biofilm anodes and the strategies to
82 adapt these biofilms to real AD process conditions. In particular, the effect of biofilm age as well
83 as presence and activity of methanogens on the biofilm stability was studied. Biofilm age is of
84 specific interest, as it alters the composition and activity of electroactive biofilms[38]. Several shock
85 and adaptation experiments using AD effluents in different concentrations (0% - 100%), filtration,
86 and inhibition of methanogens using 2-BES[39] were performed on *Geobacter* spp. dominated
87 biofilm anodes of different age. Potential inhibition of syntrophic acetogenic bacteria or
88 electroactive bacteria by 2-BES[39,40] is taken into account in the discussion of the results including
89 control measurements.
90

91 **Material and Methods**

92 All reported potentials refer to the Ag/AgCl sat. KCl reference electrode (+ 0.197 V vs. standard
93 hydrogen electrode (SHE)). All chemicals were analytical or biochemical grade. Experiments were
94 performed as independent biological in triplicates (n = 3). In total, 141 independent biofilm
95 experiments were conducted.

96 - **Experimental setup**

97 The experimental setup (Figure S1) consisted of a three-electrode setup, integrated into 250 mL
98 three-neck round bottom flasks that were used as single-chamber microbial electrolysis cells
99 (MEC). The working and the counter electrodes were made of graphite rods (anode: d = 10 mm,
100 L = 20 mm, A = 7.1 cm^2, cathode: d = 10 mm, L = 30 mm, A = 10.2 cm^2, quality CP-2200, CP-
101 Graphitprodukte GmbH, Germany). The graphite rods were connected to current collectors made
102 of stainless steel (d=0.5 mm, Goodfellow GmbH, Germany) using epoxy glue (Toolcraft, Conrad

103 Electronic SE, Germany). The current collectors were isolated with a shrink tube made of modified
104 polyolefin (ABB Ltd, Switzerland) that were fixed to the electrode using epoxy glue. The three-
105 neck round bottom flasks were closed with silicon and chloroprene stoppers. To avoid
106 overpressure due to the production of gas (H_2, CO_2, CH_4), hollow needles connected to tygon®-
107 tubes (E 3603, inner d: 1.6 mm, Saint - Gobain Performance Plastics, France) were inserted in the
108 stoppers. The produced gas was released continuously into serum bottles, half filled with distilled
109 water serving as a water lock.

110 - **Media and Inoculum**

111 The growth media was a phosphate buffer adjusted at pH 7 amended with vitamins and trace
112 elements[42,43]. Sodium acetate was used as sole carbon source and electron donor. The media
113 contained: 2.69 g L^{-1} $NaH_2PO_4.H_2O$, 5.43 g L^{-1} $Na_2HPO_4.2H_2O$, 0.31 g L^{-1} NH_4Cl, 0.13 g L^{-1}
114 KCl, 0.82 g L^{-1} $CH_3COONa \times 3H_2O$, 12.5 ml L^{-1} vitamin solution, 12.5 ml L^{-1} trace element
115 solution[42]. Vitamin solution, trace mineral solution and a 2 mol L^{-1} acetate stock solution were
116 stored at 4 °C and added just before the start of the experiments. The medium was purged with
117 nitrogen gas (Nitrogen 5.0, Linde AG, Germany) for 30 minutes prior to each experiment to ensure
118 anaerobic conditions.

119 Re-suspended, wastewater-derived *Geobacter* spp. dominated biofilm anodes were used as
120 inoculum for all experiments. The inoculum biofilms were initially grown according to
121 Gimkiewicz *et al.* [42] using wastewater from of a primary clarifier of a local wastewater treatment
122 plant (AZV Parthe, 04551 Borsdorf, Germany) followed by an electrochemical enrichment
123 according to Liu *et al.* [44]. In more detail, 50 ml L^{-1} of primary waste water were used to inoculate
124 growth medium supplemented with 10 mmol L^{-1} of sodium acetate. The biofilms obtained where
125 scratched from the anode using a spatula, suspended in fresh growth medium, and thus served as

126 inoculum for a second inoculation of a fresh graphite anode. Repeating this electrochemical
127 enrichment procedure at least three times yields *Geobacter* spp. dominated biofilms[42,44].

128 - **Biofilm formation and maturation**

129 Electroactive biofilms were grown under anaerobic conditions by inoculating the growth medium
130 with re-suspended *Geobacter* spp. dominated biofilm anodes. The electrochemical cells were
131 placed into an incubator hood (Unihood 650, UniEquip, Germany) at a temperature of 38°C to
132 resemble mesophilic AD conditions. To maintain homogeneity and reduce mass transfer
133 limitations, the media was stirred using a magnetic stirrer (Variomag Poly 15, Thermo Scientific,
134 USA) at 250 rpm. All MECs were connected to a multipotentiostat (AUTOLAB 10, EcoChemie,
135 The Netherlands for biofilm growth and PARSTAT MC, AMETEK Inc., USA for the
136 experiments).

137 Biofilm formation was performed in MEC using consecutive and repeated cycles of
138 chronoamperometry (CA) at 0.2 V for ~23 h followed by three cycles of cyclic voltammetry (CV)
139 with vertex potentials at –0.5 V and 0.3 V and a scan rate of 1 mV s^{-1}. Depending on the
140 experiment, less mature and more mature biofilms were grown in batch mode. These are further
141 denominated as "young biofilm" for a pre-growth over a period of three weeks and "old biofilm"
142 for five weeks pre-growth, respectively. Commonly one batch cycle was lasting one week,
143 regardless of the residual acetate concentration in order to always ensure its sufficient availability.

144 - **AD effluent**

145 AD effluent was taken from a mesophilic, semi-continuous 12 L up-flow fixed bed reactor,
146 operated on a hemicellulose fraction originating from a pulping process. The AD reactor setup
147 (Figure S2), operation conditions, process parameters as well as composition of the used AD
148 effluent (Table S1) is provided in the SI.

- **Experiments**

Pre-grown biofilm anodes were used for five sets of experiments that are summarized in Table 1. All experiments were conducted in batch mode with one batch lasting one week. Two additional batches denoted as controls were conducted with young and old biofilms with only growth medium amended with vitamin, trace element and acetate as electron donor. Regardless the AD effluent concentration in the growth medium, 12.5 ml L^{-1} vitamin solution, 12.5 ml L^{-1} trace element solution and 10 mmol L^{-1} acetate were always added before the start of each batch.

Table 1. Parameters of the performed experiments.

Name of the experiment	Age of the biofilms / weeks	AD effluent concentration in the growth media / % (v/v)	New biofilms for each AD effluent concentration	Duration / batch cycles (weeks)
AD shock young	3 (young)	0, 10, 25, 50, 75, 100	Yes	2
AD shock old	5 (old)	0, 10, 25, 50, 75, 100	Yes	2
AD adaptation	5 (old)	0, 10, 25, 50, 75, 100	No	2
2-BES	5 (old)	50	No	4
Filtration	5 (old)	50	No	5

First, shock experiment with young and old biofilms were performed to examine the effect of the biofilm age on its resistance. For shock experiments, the biofilms were exposed to different concentrations of AD effluent for two batch cycles (Table 1, AD shock young/old). Furthermore, during adaptation experiments, old biofilms were exposed stepwise to increasing concentrations of AD effluent (Table 1, AD adaptation).

To evaluate the interaction between methanogens in AD effluent and *Geobacter* spp. dominated biofilms, a fixed concentration of AD effluent (50 %) pre-treated with 50 mmol L^{-1} sodium 2-bromoethanesulfonate[39,45] (2-BES, 98 %, Sigma-Aldrich, China) was applied to old biofilms (Table 1, 2-BES). For pre-treatment, the mixture of AD effluent, growth medium and 2-BES was incubated under anaerobic conditions for 24 h at 6°C and adapted to room temperature before use.

168 Finally, a filtration step was applied to the AD effluent to examine the effect of removal of
169 particles and microorganisms from AD effluent on old biofilms (Table 1, Filtration). Filtration of
170 AD effluent was conducted stepwise using cellulose acetate filter papers with three different pore
171 sizes (1.2 µm, 0.45 µm and 0.2 µm, Sartorius Stedim Biotech GmbH, Germany).
172 Since the AD effluent had a low concentration of VFA, 10 mmol L^{-1} acetate was added throughout
173 all experiments to assure sufficient supply with electron donor and carbon source (see also Table
174 S1).

175 - **Analysis**

176 Biofilm activity was monitored by CA and CV measurements as described above (CA for ~23 h
177 followed by three CV cycles). CV measurements were analyzed towards 1) overall changes of
178 maximum current density ($j_{max,}$) and 2) changes in the formal potential (E_f) of the extracellular
179 electron transfer site (cytochromes). For the latter, the 1st derivative of selected CV scans were
180 examined (only 3rd cycle and only one out of three replicates from the beginning of a batch cycle).
181 CA data was analyzed towards 1) j_{max} and 2) coulombic efficiency (CE, percentage of the electrons
182 present in the substrate acetate that is recovered as current[8,46]). Maximum current density was
183 reported by normalizing the maximum current to the projected surface area of the working
184 electrode (mA cm^{-2}). CE was determined for each batch cycle using equation (1).

185 $$CE = \frac{M_{Ac} \int idt}{zFV\Delta c} \times 100 \quad (1)$$

186 M_{Ac} = 59.04 g mol^{-1} is the molar mass of acetate, V = 250 mL is the buffer volume in the MEC, F
187 is the Faraday constant (F = 96485.34 C mol^{-1}), z = 8 is the released number of electrons during
188 oxidation of acetate, $\Delta c = c_0 - c_1$ is the difference in exact acetate concentration that is acetate
189 consumption in g L^{-1} (method described below) and $\int idt$ the transferred charge, calculated by
190 integrating the current over time [42].

191 The exact acetate concentration that is preexistent plus spiked acetate was determined by high
192 performance liquid chromatography (HPLC, Model CBM-20A, Shimadzu, USA) equipped with a
193 refractive index detector RID 20A, a prominence diode array detector SPD.M20A and a CTO-
194 20AC prominence column oven. 5 mmol L^{-1} sulfuric acid was used as isocratic mobile phase with
195 a flow rate of 0.5 mL min^{-1} at 50 °C, over a total run time of 30 min. 1 mL of media was taken
196 from each electrochemical cell at the beginning and end of each batch cycle. The samples were
197 centrifuged at 10.000×g for 10 min and filtered using a 0.2 µm syringe filter (Nylon, VWR,
198 China). The samples were stored at -20 °C until measurement.
199 Beside continuous electrochemical characterization and acetate measurement, headspace gas
200 composition in each electrochemical cell was determined at the end of each batch cycle to check
201 for differences in methane production in the replicates and the different conditions. Therefore,
202 1 mL gas samples were taken from the headspace of the MECs using a syringe. The samples were
203 injected into glass vials pre-flushed with argon (Argon 4.8, Linde AG, Germany). Gas composition
204 was measured using a gas chromatograph (GC) equipped with an autosampler (Perkin Elmer Inc,
205 Waltham, USA). The GC was equipped with HayeSep N/Mole Sieve 13X columns and a thermal
206 conductivity detector. The oven and detector temperatures were 60 °C and 200 °C, respectively.
207 The carrier gas was argon. Every gas sample was analyzed within 24 h after sampling.
208 Furthermore, NH_4^+-N (colorimetric Nessler test[47], Photometer Hach DR 3900), pH (pH 3310,
209 WTW, Germany) and conductivity of the media (Cond 3110, WTW, Germany) were measured
210 prior and after each batch cycle.

211 - **Statistical Analysis**

212 For statistical analysis, confidence interval (CI) at 95 % confidence was used to deduce significant
213 differences of different treatments within one experiment, this is indicated by non-overlapping CI

214 bars in the graphs. Additionally, one-way analysis of variance (ANOVA) with post-hoc Tukey test
215 at the significance level $\alpha = 0.05$ was performed (Origin Version 2021, OriginLab Corporation,
216 Northampton, MA, USA,Version 9.8.0.200) to assess significant differences between experiments
217 conducted under different conditions, e.g. AD shock young/old or filtration/2-BES experiment.
218 CE and j_{max} of first week's batches were compared with each other as well as second week's
219 batches, respectively.

220 **Microbial community analysis**

221 At the end of the two batches (shock experiment) and at the end of all batches (adaptation, 2-BES
222 and filtration experiments) biofilms from each of the three independent replicates were harvested
223 from the electrode surface using a spatula. The biofilms were put into 2 mL microcentrifuge tubes,
224 spinned down at 10.000×g for 10 min (centrifuge 5430 R, Eppendorf AG, Germany) and stored at
225 -20 °C until analysis. Microbial community analysis (18 samples) was performed on DNA level
226 to determine changes in the bacterial communities during the experiments. DNA extraction was
227 performed with the NucleoSpin Soil® kit (Macherey-Nagel) following the manufacturer's
228 instruction. Terminal restriction fragment length polymorphism (T-RFLP) analysis was based on
229 partial amplification of the 16S rRNA gene according to standard procedures as described by Koch
230 *et al.* [48]. PCR was performed with the Fluorescein-amidite labelled primer set UniBac27f and
231 Univ1492r, and restriction digestion using RsaI and HaeIII.

232

233 **Results and discussion**

234 - **AD shock on young and old: The effect of age on biofilm resistance**

235 Figure 1 shows the CE and j_{max} observed for young and old biofilms after being exposed to AD
236 effluent of different concentration (see also Table 1, AD shock young/old). CE values higher than

237 100% are a consequence of the used one-chamber configuration[49]. Hydrogen from the cathode is
238 used as substrate either by methanogens[50,51] or *Geobacter* spp.[52]. Therefore more electrons are
239 transferred to the anode than can be derived from oxidation of acetate leading to a CE > 100% [52].
240 Furthermore, residual acetate and other VFA in the AD effluent can bias the CE that is calculated
241 on total acetate only (see also Table S1).

242 Figure 1a shows that CE as well as j_{max} of young biofilms decreased significantly during the second
243 batch cycle using 25%, 50%, 75% and 100% AD effluent. Visual examination of the biofilms after
244 the end of the second batch cycle provided evidence that the biofilms detached from the electrode
245 surface and moved into the planktonic phase (Figure S3a). Only during experiments with 10% AD
246 effluent, no significant loss of the CE and j_{max} of young biofilms was observed during the second
247 batch cycle. Therefore, it was decided to continue this experiment for two more batch cycles. From
248 the third batch cycle onwards, both CE and j_{max} also dropped significantly, indicating the same
249 behavior as described for higher AD effluent concentrations (Figure S4a). The CE at the end of
250 the fourth batch cycle was 12.53±12.10%. When considering the value at the end of the first batch
251 cycle of 102.93±3.57% this indicates a drop by factor 8.2±3.4 which corresponds to a loss of ~88%
252 of the biofilm activity based on the CE. Similar behavior was observed with j_{max} for the same
253 concentration which decreased from 0.63±0.07 mA cm^{-2} (first batch cycle) to 0.12±0.08 mA cm^{-2}
254 (fourth batch cycle) corresponding to a drop by factor 5.4±1.1 which indicates a loss of ~81% of
255 the biofilm activity based on j_{max}. Thus, for young biofilms, the transition from biofilm to the
256 planktonic state seems to be the main reason for the loss of electrochemical biofilm activity when
257 being exposed to AD effluent (Figure S4b) which is in line with previous observations[23].

258 Figure 1b shows the average CE and j_{max} observed for old biofilms during the same shock
259 experiments as described above for young biofilms. In contrast to young biofilms, the performance

260 of old biofilms was maintained for each used AD concentration. In comparison to the CE at the
261 end of the first batch cycle, the value at the end of the second batch cycle sometimes increased,
262 e.g., 75% and 100% AD effluent, albeit insignificantly. This increase could also be caused by
263 slightly increased VFA concentrations in AD effluent (see Table S1).

264 Noteworthy, old biofilms remained intact on the electrode surface (Figure S3b), clearly indicating
265 that a maturing period of additional 2 weeks or 5 weeks in total improves the resistance that is the
266 ability of *Geobacter* spp. dominated biofilms to resist against inhibition by components originating
267 from AD effluent compared to young biofilms that have been grown for 3 weeks, only.

268 Turnover CVs of young biofilms in Figure S5a reveal a formal potential of an electron transfer site
269 of E_f = -0.35±0.01 V (data calculated from CVs taken after the first batch cycle for 10%, 25%,
270 50%, 75% and 100% AD effluent). This data is in good accordance with literature data on turnover
271 CVs of *Geobacter sulfureducens* biofilms[53] and most likely shows the outer membrane
272 cytochrome OmcB. In the second week of exposure to AD effluent of the young biofilms, the
273 current and hence the peak of the first derivative for each single concentration dropped, except in
274 the case of 10% AD effluent, making it impossible to determine a defined E_f (see Figure 1a & S5a).
275 It was also impossible to determine a distinct E_f in old biofilms (Figure S5b). Here, the
276 identification of a single redox system was not possible due to increased peak width and shift to
277 higher potentials, maybe caused by increased presence of redox active molecules that are not
278 necessarily involved in extracellular electron transfer. This likely increase in redox active
279 molecules can be the result of a higher amount of extracellular polymeric substances that are more
280 abundant in old biofilms compared to young biofilms[54].

281 Using ANOVA to compare CE and j_{max} of the first and the second batch cycles of AD shock young
282 and AD shock old experiments (from 10% AD effluent concentrations onwards) showed p values
283 higher than α when comparing the first batches and p values lower than α when comparing the
284 second batches (Figure S8). This means that at the significance level of α=0.05, the population
285 means are not significantly different in the first batches, but in the second batches. In other words,
286 regardless of the AD effluent concentration, first batches show no influence of AD effluents on
287 the biofilm activity. The results from this experiment show that old *Geobacter* spp. dominated
288 biofilm anodes are by far more resistant towards AD effluent, indicated by no significant difference
289 in CE and j_{max} values from the first to the second batch cycle in contrast to CE and j_{max} for the
290 experiment using young *Geobacter* spp. dominated biofilm anodes. A reason for the observed
291 behavior could be that complex microbial communities can be formed[55–57]. In this complex
292 microbial community, for instance, fermentative bacteria and non-planktonic methanogens
293 dominate the outer layers of the biofilm electrode, which means that in older biofilms they are
294 more prominent, thus possibly protecting the electroactive bacteria located in the inner layers to a
295 certain extend from potential inhibitors or alternative electron acceptors present in the AD
296 effluent[37]. Another reason could be the higher abundance of extracellular polymeric substance in
297 old biofilms that protect the bacteria from unfavorable environmental conditions[54].

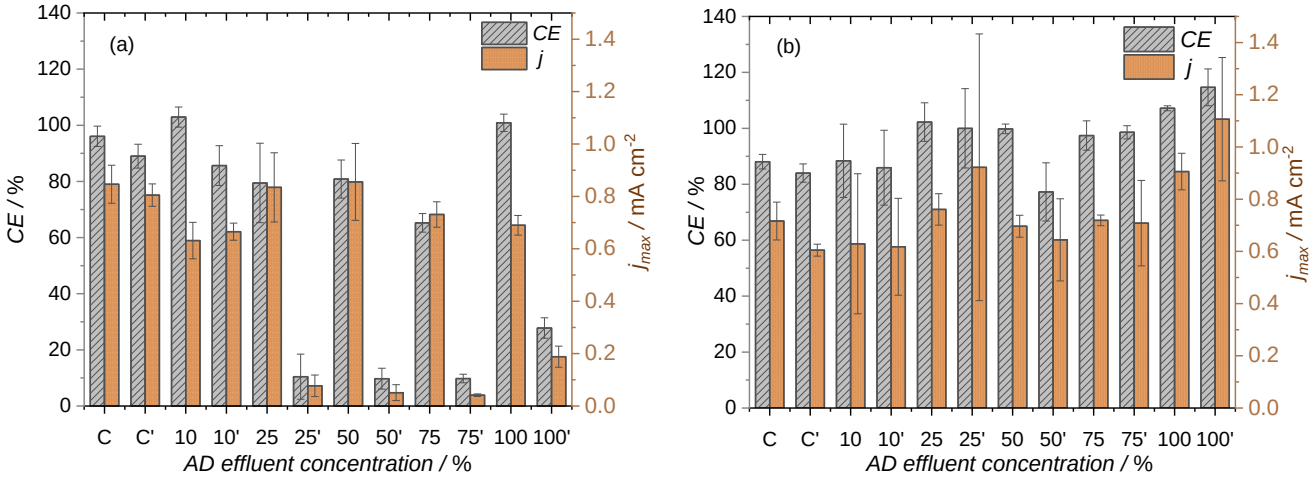

Figure 1. CE and j_{max} during: (a) shock experiments with young biofilms (Table 1, AD shock young) (b) shock experiments with old biofilms (Table 1, AD shock old). C: control with only acetate as carbon source, ' indicates second week (second batch), n=3, error bars indicate CI.

- **Increasing resistance of mature electroactive biofilms without adaptation**

Figure 2 shows the average CE and j_{max} observed when old biofilms were subsequently exposed to increasing concentrations of the AD effluent (10% - 100%, see also Table 1, AD adaptation). The biofilm activity in terms of CE and j_{max} remains stable when using 10% and 25% AD effluent. From the first week of 50% AD effluent concentration onwards, both CE and j_{max} gradually decrease. The CE calculated for experiments using 100% AD effluent (of 2.74±0.81%) dropped by ~97% compared to the CE of the control (88.08±2.61%). Visual examination of the biofilms revealed electrodes with massive biofilm detachment, similar to the shock experiments with young biofilms (Figure S3a). Therefore, biofilm adaptation to AD effluent was not successful but old biofilms remained active for 4 more weeks when being exposed to up to 25% AD effluent, which is 2 weeks more compared to young biofilms in the AD shock experiments. Their performance gradually decreased when exposed to AD effluent concentrations > 25%.

The CV measurements of the biofilms of the most defined peaks of the adaptation experiment (10% and 25% AD effluent) show a E_f at -0.340±0.006 V (Figure S6) that is comparable to the E_f observed for young biofilms (Figure S5a). Calculation of E_f for other AD effluent concentration was not possible as the first derivatives showed no defined peaks. The peak intensity gradually decreased over time, indicating a concomitant loss of the biofilm from the electrode (Figure S6), albeit not suddenly, rather gradually.

The electroactive biofilm anodes have shown only a limited stability in AD effluent. However, the exact cause of the observed biofilm loss or inactivation is still unclear. It seems that components of the AD effluent interact with the electroactive bacteria in the biofilm and cause a dispersal of bacteria from the biofilm into the planktonic phase. Old biofilms can withstand longer than young biofilms, and we speculate that it is due to a more pronounced protective or shielding layer of microorganisms (bacteria and archaea) on the outer layers of the biofilm. Beside protecting the EAM against toxic compounds or grazing protozoans[58], such a layer may limit the interaction of *Geobacter* spp. with alternative TEA, e.g., methanogens in terms of direct interspecies electron transfer[59], solid mineral particles or dissolved compounds, that may cause an interaction leading to detachment. TEA may allow the bacteria to live in a planktonic state gaining access substrate and limiting negative aspects of living in a biofilm, e.g., pH-shift due to high proton and CO_2 concentration at the surface of the electrode (thermodynamic limitations due to high product concentration and low pH), substrate mass transfer limitations as well as competition for substrate in general[33]. However, potential interaction between *Geobacter* spp. dominated biofilms and, e.g., TEA or grazing protozoans as reported for electroactive biofilms[58] have not been studied here and therefore, one may speculate that these also contribute to the observed loss of activity.

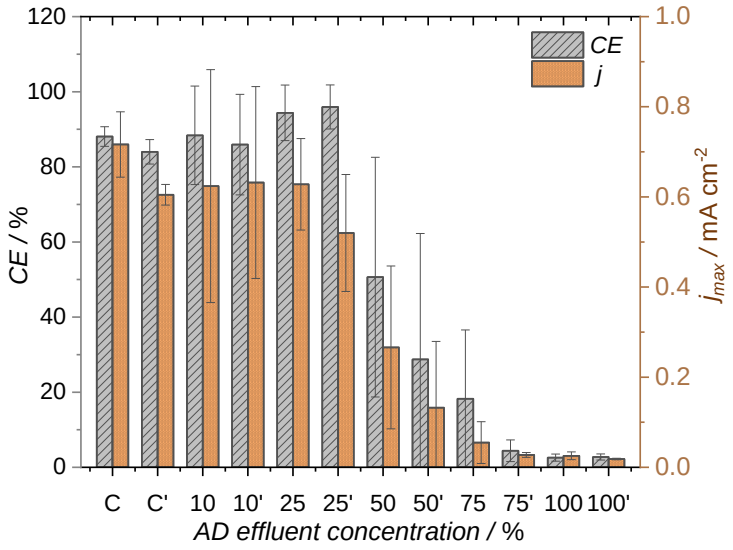

Figure 2. CE and j_{max} during stepwise adaptation of old biofilms from 10% to 100%, each concentration run for two batch cycles (Table 1, AD adaptation). C: control with only acetate as carbon source, ': second week (second batch), n=3 and error bars indicate the CI.

- **Do methanogens affect the electrochemical performance of *Geobacter* spp. dominated biofilms**

For investigating the hypothesis that methanogens and/or solid particles present in the AD effluent cause the observed loss of activity or biofilm of *Geobacter* spp. dominated biofilm anodes, further experiments using old biofilms were conducted: (1) the activity of methanogens in the AD effluent was inhibited using 50 mmol L^{-1} 2-BES and (2) methanogens and solid particles were excluded by filtration. As shown in Figure 1 and Figure 2, 50% AD effluent causes a decrease of biofilm activity of young and old biofilms, even if old biofilms are able to withstand the inhibitory effects of AD effluent for a period of ≥4 weeks. Figure 3a shows the average CE and j_{max} of old biofilms when exposed to 50% AD effluent treated with 50 mmol L^{-1} 2-BES. Here, CE and j_{max} do not significantly change, as inhibition of methanogens using 2-BES prevents loss of biofilm activity or biofilm from the anode. In contrast to shock and adaptation experiments, where CH_4 production

351 was always observed (see Figures S7a, S7b and S7c), no CH_4 was detected after application of 2-
352 BES (Figure S7d, red squares). This indicates a complete inhibition of methanogens by 2-BES.
353 Therefore, it is more than likely that methanogens have a negative influence on young and old
354 biofilms in terms of j_{max} and CE. The observed increase of CE to values >100% during application
355 of 50% AD effluent can thus likely be attributed to bacteria in the AD effluent that contribute to
356 substrate formation, e.g., acetate via homoacetogenesis or utilization of hydrogen produced at the
357 cathode or by syntrophic bacteria. For instance, Li *et al*. proposed a similar reasoning, showing
358 that EAM can use certain fatty acids when they are not hindered by substrate-competing processes
359 such as methanogenesis[9]. Furthermore, application of 2-BES inhibits methanogens present in the
360 biofilm. As reported by Rozendal *et al.* [4], mainly hydrogenotrophic methanogens colonize the
361 upper part of the anodic biofilms, where they generate CH_4 from electron donors such as H_2 or
362 acetate and therefore, competing with *Geobacter* spp. in the deeper parts of the biofilms. Since
363 non-planktonic and planktonic methanogens were completely inhibited during the application of
364 2-BES, substrate competition was circumvented and all of the acetate and H_2 produced at the
365 cathode could be used as electron donor by the EAM, hence the high CE observed[45,49].

366 According to Figure 3b, the filtration and therefore the exclusion of bacteria, archaea and/or
367 particles with a diameter >0.2 µm from the AD effluent also prevents the prior observed loss of
368 biofilm or reduced biofilm activity. The CE was constant over the 5 batch cycles with a mean value
369 of 101.8 ± 2.5 % that is much more homogenous compared to the experiment using 2-BES
370 (Figure 3a). However, a slight increase in j_{max} was observed in figure 3b, which may be a result of
371 increased acetate availability by acetogenesis from remaining VFA in the AD effluent. Adding 2-
372 BES also inhibits syntrophic acetogenic bacteria responsible of acetogenesis as described
373 elsewhere[39,40]. We can exclude inhibition of the biofilms by application of 50 mmol L^{-1} 2-BES to

374 a certain extend as we performed a control measurement using old *Geobacter* spp. dominated
375 biofilms in combination with 50 mmol L^{-1} BES that shows no significant inhibition of the biofilm
376 activity for a period of two batches (two weeks, see Figure S10). Therefore, the difference in j_{max}
377 between the figure 3a and 3b can be related to the fact that filtration excludes potential inhibitors
378 without influencing syntrophic acetogenic bacteria.

379 Using ANOVA to compare CE and j_{max} of the experiment performed with 2-BES and filtration at
380 0.2µm showed p values lower than α (Figure S9). This means that at the significance level of
381 α=0.05, the population means are significantly different, although both pretreatments contribute to
382 increase the resistance of the biofilms. In other words, at 50% AD effluent concentration, the
383 biofilm activity is not affected when applying 2-BES and microfiltration, even if the population
384 mean differs.

385 The results shown in Figure 3 lead to the conclusion that methanogens and/or solid particles
386 >0.2 µm in the AD effluent induce the observed inhibition of *Geobacter* spp. dominated biofilm
387 anodes. As CH_4 was detected in the headspace at the end of each batch cycle of the filtration
388 experiment (Figure S7d, black squares) it is reasonable to assume that methanogens present in the
389 biofilms are responsible for the observed methane production. To provide a detailed picture on the
390 exact mechanisms, experiments using effluent from other AD processes accompanied with a
391 detailed qualitative and quantitative analysis of the microbiological community in the biofilm and
392 the bulk liquid are required.

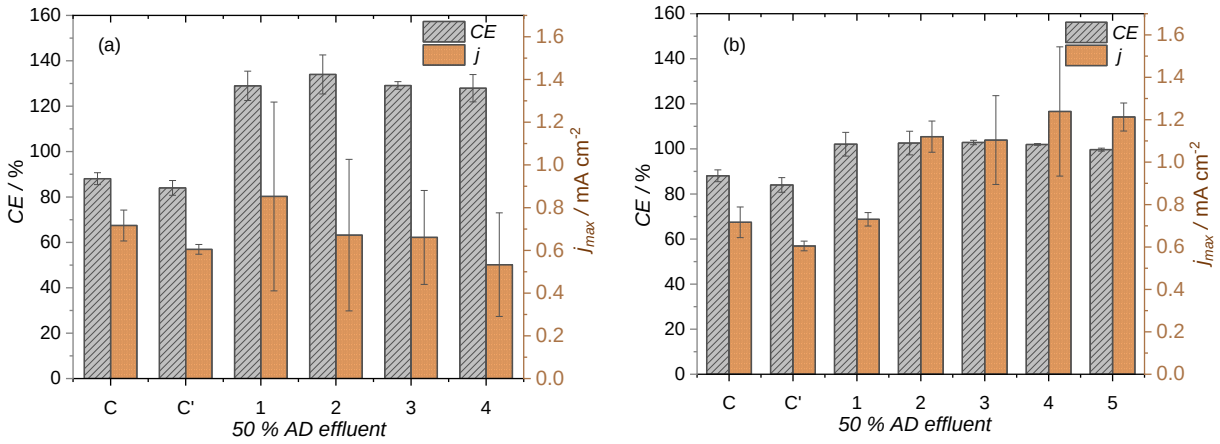

Figure 3. CE and j_{max} during: (a) 2-BES application to inhibit methanogens (Table 1, 2-BES), (b) AD effluent filtration at 0.2 µm to remove solid particles and microorganisms (Table 1, Filtration). C: control with only acetate as carbon source, ' indicate second week (second batch), 1, 2, 3, 4 and 5 indicate the successive batch cycles with 50% AD effluent, n=3 and error bars indicate the CI.

- **Microbial community analysis**

To monitor the changes in the composition of electroactive biofilms induced by AD effluent in all experiments presented above, TRFLP analysis[60] of the bacterial 16s RNA gene in biofilms was performed at the end of each experiment. The results were compared to the composition of the primary *Geobacter* spp. inoculum. Figure 4 shows the relative abundance (RA) of *Geobacter* spp. on the biofilm anodes. According to other studies *Geobacter* spp. can be assigned to TRF (239)240 for Rsa I [61]. Analysis of the inoculum (control) indicated that *Geobacter* spp. accounts for 81.42±13.55% RA and only about 18.58% RA for other bacteria that were not further analysed. RA of *Geobacter* spp. dropped to, e.g., 3.42±3.38% after the shock experiment using 75% AD effluent in combination with young biofilms (Table 1, AD shock young). This reduced RA is rather due to the observed biofilm loss than a real change of the microbial community in the biofilm. The more resistant old biofilms show, e.g., 70.78±4.66% RA of *Geobacter* spp. in AD shock

409 experiments with old biofilm using 75% AD effluent. In combination with the visual examination
410 of the biofilm electrodes at the end of the experiments (Figure S3), the results confirm that the
411 inhibitory effect of the AD effluent on the integrity and community structure is more pronounced
412 for young biofilms than for old biofilms.

413 Analysis of samples taken from the anodes at the end of the AD adaptation experiments (Table 1)
414 show nearly no RA of *Geobacter* spp., supporting again the results of the visual examination that
415 showed total loss of electroactive biofilm from the electrode. Therefore, bacteria attached to the
416 electrodes surface that were scraped off might be other microbial species not involved in current
417 generation or simply bacteria from the planktonic phase that remained and thus apparently
418 accumulated during biofilm dispersal.

419 By inactivating and minimizing methanogens using 2-BES and filtration, respectively (see Table
420 1), the RA of *Geobacter* spp. remained almost identical compared to the control (inoculum). RA
421 of *Geobacter* was 75.99±1.48% and 80.01±9.61% respectively for both cases. Therefore, the
422 results of this study show that methanogens and/or particles with diameter >0.2 µm present in the
423 AD effluent have a distinct influence on the activity, stability as well as the microbial community
424 of *Geobacter* spp. dominated biofilm anodes. The question, if *Geobacter* spp. is still active in the
425 planktonic phase cannot be answered here, since the medium of each cell was changed at the end
426 of each batch cycle, making it inappropriate to specifically quantify the biofilm loss over each
427 batch cycle and hence whether and for how long EAM might remain active in the planktonic phase.
428 This would require, e.g. daily or at least weekly quantitative analysis such as RT–qPCR.

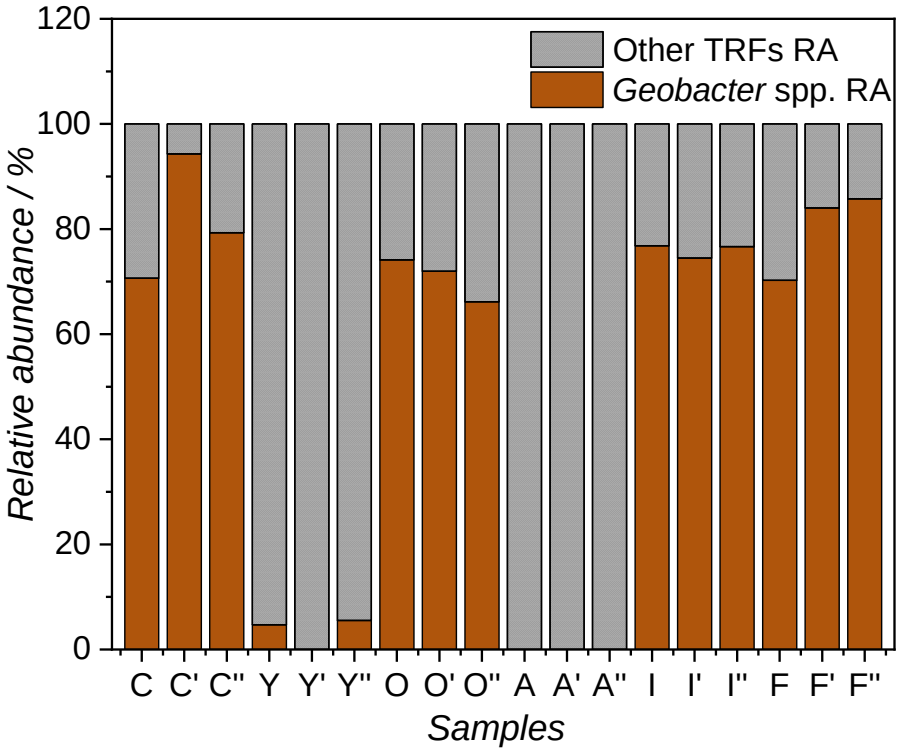

Figure 4. Microbial community taxonomic plots based on the mean relative abundance of the16S rRNA gene. C: primary inoculum (control), Y: AD shock with 75% AD effluent and young biofilms (Figure 1a), O: AD shock with 75% AD effluent and old biofilms (Figure 1b), A: AD adaption experiments with old biofilms (Figure 2), I: inhibition experiment with 2-BES using old biofilms (Figure 3a), F: Filtration experiments with old biofilms (Figure 3b), ’ and " indicate independent biological replicates, Brown: *Geobacter* spp., Misc colors: others TRFs.

AUTHOR INFORMATION

Corresponding Author

*Jörg Kretzschmar

E-Mail: joerg.kretzschmar@dbfz.de

Author Contributions

The manuscript was written through contributions of all authors. All authors have given approval to the final version of the manuscript. The authors contributed as follows:

Conceptualization: DND, JK, FH

Investigation: DND

Formal analysis: DND, JK, FH

Funding Acquisition: DND, JK, FH

Supervision: JK, FH

Visualization: DND

Writing – Original Draft Preparation: DND

Writing – Review & Editing: DND, JK, FH

Acknowledgements

The authors especially thank Anne Kuchenbuch for technical assistance during molecular biological analysis and Sophie Reinisch for support in the compilation of the graphical abstract. DND gratefully acknowledges funding by the PhD student program of the DAAD (German academic exchange service, 57381412). JK acknowledges funding by the federal ministry of economic affairs and energy (Project “Optimand”, grant number: 03KB115) and funding by the federal ministry of education and research (Project “BioFavor”, grant number: 031B0483E). This work was supported by the Helmholtz-Association within the Research Programme Renewable Energies.

Abbreviations

AD anaerobic digestion; MET microbial electrochemical technology; MEC microbial electrolysis cell; 2-BES 2-bromoethanesulfonate; CA chronoamperometry; CV cyclic voltammetry; j_{max} maximum current density; CE coulombic efficiency; HPLC High Performance Liquid Chromatography; T-RFLP Terminal restriction fragment length polymorphism; PCR polymerase chain reaction; CI confidence interval; n number of replicates; TEA terminal electron acceptor; EAM electroactive microorganisms; DIET direct interspecies electron transfer; ANOVA analysis of variance; VFA volatile fatty acids.

Supporting Information.

Description of experimental setup and operation of AD reactors, biofilm detachment, 1st derivatives of CVs, methane concentration in the headspace of the MECs.

References

(Ohne Gruppe)

(1) Fabien Monnet. An Introduction to Anaerobic Digestion of Organic Wastes. *Final Report* **2003**, 1–48.

(2) Meegoda, J. N.; Li, B.; Patel, K.; Wang, L. B. A Review of the Processes, Parameters, and Optimization of Anaerobic Digestion. *International journal of environmental research and public health* **2018**, *15,* DOI: 10.3390/ijerph15102224.

(3) Schröder, U.; Harnisch, F.; Angenent, L. T. Microbial electrochemistry and technology: Terminology and classification. *Energy Environ. Sci.* **2015**, *8*, 513–519.

(4) Rozendal, R. A.; Hamelers, H. V. M.; Rabaey, K.; Keller, J.; Buisman, C. J. N. Towards practical implementation of bioelectrochemical wastewater treatment. *Trends in biotechnology* **2008**, *26*, 450–459.

(5) Fornero, J. J.; Rosenbaum, M.; Cotta, M. A.; Angenent, L. T. Carbon dioxide addition to microbial fuel cell cathodes maintains sustainable catholyte pH and improves anolyte pH, alkalinity, and conductivity. *Environmental science & technology* **2010**, *44*, 2728–2734.

(6) Logan, B. E.; Hamelers, B.; Rozendal, R.; Schröder, U.; Keller, J.; Freguia, S.; Aelterman, P.; Verstraete, W.; Rabaey, K. Microbial fuel cells: Methodology and technology. *Environmental science & technology* **2006**, *40*, 5181–5192.

(7) Logan, B. E.; Call, D.; Cheng, S.; Hamelers, H. V. M.; Sleutels, T. H. J. A.; Jeremiasse, A. W.; Rozendal, R. A. Microbial electrolysis cells for high yield hydrogen gas production from organic matter. *Environmental science & technology* **2008**, *42*, 8630–8640.

(8) Ledezma, P.; Kuntke, P.; Buisman, C. J. N.; Keller, J.; Freguia, S. Source-separated urine opens golden opportunities for microbial electrochemical technologies. *Trends in biotechnology* **2015**, *33*, 214–220.

(9) Li, X. M.; Cheng, K. Y.; Wong, J. W. C. Bioelectricity production from food waste leachate using microbial fuel cells: Effect of NaCl and pH. *Bioresource technology* **2013**, *149*, 452–458.

(10) Waqas, M.; Rehan, M.; Aburiazaiza, A. S.; Nizami, A. S. Wastewater Biorefinery Based on the Microbial Electrolysis Cell: Opportunities and Challenges. *Progress and Recent Trends in Microbial Fuel Cells*; Elsevier, 2018; pp 347–374.

(11) Barbosa, S. G.; Peixoto, L.; Ter Heijne, A.; Kuntke, P.; Alves, M. M.; Pereira, M. A. Investigating bacterial community changes and organic substrate degradation in microbial fuel cells operating on real human urine. *Environ. Sci.: Water Res. Technol.* **2017**, *3*, 897–904.

(12) Wang, X.; Aulenta, F.; Puig, S.; Esteve-Núñez, A.; He, Y.; Mu, Y.; Rabaey, K. Microbial electrochemistry for bioremediation. *Environmental Science and Ecotechnology* **2020**, *1*, 100013.

(13) Vrieze, J. de; Arends, J. B. A.; Verbeeck, K.; Gildemyn, S.; Rabaey, K. Interfacing anaerobic digestion with (bio)electrochemical systems: Potentials and challenges. *Water research* **2018**, *146*, 244–255.

(14) Luo, H.; Liu, G.; Zhang, R.; Bai, Y.; Fu, S.; Hou, Y. Heavy metal recovery combined with H_2 production from artificial acid mine drainage using the microbial electrolysis cell. *Journal of hazardous materials* **2014**, *270*, 153–159.

(15) Song, Y.-H.; Hidayat, S.; Kim, H.-K.; Park, J.-Y. Hydrogen production in microbial reverse-electrodialysis electrolysis cells using a substrate without buffer solution. *Bioresource technology* **2016**, *210*, 56–60.

(16) Jeremiasse, A. W.; Hamelers, H. V.M.; Saakes, M.; Buisman, C. J.N. Ni foam cathode enables high volumetric H2 production in a microbial electrolysis cell. *International Journal of Hydrogen Energy* **2010**, *35*, 12716–12723.

(17) Hidayat, S.; Song, Y.-H.; Park, J.-Y. Performance of a continuous flow microbial reverse-electrodialysis electrolysis cell using a non-buffered substrate and catholyte effluent addition. *Bioresource technology* **2017**, *240*, 77–83.

(18) Luo, H.; Jenkins, P. E.; Ren, Z. Concurrent desalination and hydrogen generation using microbial electrolysis and desalination cells. *Environmental science & technology* **2011**, *45*, 340–344.

(19) Lin, H.; Wu, X.; Bo Hu3. Microbial Electrochemical Systems for Agro-industrial Wastewater Remediation and Renewable Products Generation: A Review. *Microbiology and Biotechnology* **2014**, *1*, 1–20.

(20) Desloover, J.; Woldeyohannis, A. A.; Verstraete, W.; Boon, N.; Rabaey, K. Electrochemical resource recovery from digestate to prevent ammonia toxicity during anaerobic digestion. *Environmental science & technology* **2012**, *46*, 12209–12216.

(21) Sasaki, K.; Sasaki, D.; Morita, M.; Hirano, S.-I.; Matsumoto, N.; Ohmura, N.; Igarashi, Y. Bioelectrochemical system stabilizes methane fermentation from garbage slurry. *Bioresource technology* **2010**, *101*, 3415–3422.

(22) Muñoz, R.; Meier, L.; Diaz, I.; Jeison, D. A review on the state-of-the-art of physical/chemical and biological technologies for biogas upgrading. *Rev Environ Sci Biotechnol* **2015**, *14*, 727–759.

(23) Kretzschmar, J.; Böhme, P.; Liebetrau, J.; Mertig, M.; Harnisch, F. Microbial Electrochemical Sensors for Anaerobic Digestion Process Control - Performance of Electroactive Biofilms under Real Conditions. *Chem. Eng. Technol.* **2018**, *41*, 687–695.

(24) Tartakovsky, B.; Manuel, M.-F.; Neburchilov, V.; Wang, H.; Guiot, S. R. Biocatalyzed hydrogen production in a continuous flow microbial fuel cell with a gas phase cathode. *Journal of Power Sources* **2008**, *182*, 291–297.

(25) Kim, H.-W.; Nam, J.-Y.; Shin, H.-S. Ammonia inhibition and microbial adaptation in continuous single-chamber microbial fuel cells. *Journal of Power Sources* **2011**, *196*, 6210–6213.

(26) Kim, H.-W.; Nam, J.-Y.; Shin, H.-S. Ammonia inhibition and microbial adaptation in continuous single-chamber microbial fuel cells. *Journal of Power Sources* **2011**, *196*, 6210–6213.

(27) Tice, R. C.; Kim, Y. Influence of substrate concentration and feed frequency on ammonia inhibition in microbial fuel cells. *Journal of Power Sources* **2014**, *271*, 360–365.

(28) Sun, D.; Wang, A.; Cheng, S.; Yates, M.; Logan, B. E. Geobacter anodireducens sp. nov., an exoelectrogenic microbe in bioelectrochemical systems. *International journal of systematic and evolutionary microbiology* **2014**, *64*, 3485–3491.

(29) Yang, G.; Chen, S.; Zhou, S.; Liu, Y. Genome sequence of a dissimilatory Fe(III)-reducing bacterium Geobacter soli type strain GSS01(T). *Standards in genomic sciences* **2015**, *10*, 118.

(30) Roden, E. E.; Kappler, A.; Bauer, I.; Jiang, J.; Paul, A.; Stoesser, R.; Konishi, H.; Xu, H. Extracellular electron transfer through microbial reduction of solid-phase humic substances. *Nature Geosci* **2010**, *3*, 417–421.

(31) Klüpfel, L.; Piepenbrock, A.; Kappler, A.; Sander, M. Humic substances as fully regenerable electron acceptors in recurrently anoxic environments. *Nature Geosci* **2014**, *7*, 195–200.

(32) Lovley, D. R. Syntrophy Goes Electric: Direct Interspecies Electron Transfer. *Annual review of microbiology* **2017**, *71*, 643–664.

(33) Rotaru, A.-E.; Calabrese, F.; Stryhanyuk, H.; Musat, F.; Shrestha, P. M.; Weber, H. S.; Snoeyenbos-West, O. L. O.; Hall, P. O. J.; Richnow, H. H.; Musat, N. *et al.* Conductive Particles Enable Syntrophic Acetate Oxidation between Geobacter and Methanosarcina from Coastal Sediments. *mBio* **2018**, *9,* DOI: 10.1128/mBio.00226-18.

(34) Yee, M. O.; Snoeyenbos-West, O. L.; Thamdrup, B.; Ottosen, L. D. M.; Rotaru, A.-E. Extracellular Electron Uptake by Two Methanosarcina Species. *Front. Energy Res.* **2019**, *7*, 1.

(35) Dubé, C.-D.; Guiot, S. R. Ethanol-to-methane activity of Geobacter-deprived anaerobic granules enhanced by conductive microparticles. *Process Biochemistry* **2017**, *63*, 42–48.

(36) Dhar, B. R.; Lee, H.-S. Evaluation of limiting factors for current density in microbial electrochemical cells (MXCs) treating domestic wastewater. *Biotechnology reports (Amsterdam, Netherlands)* **2014**, *4*, 80–85.

(37) Kuntke, P.; Sleutels, T. H. J. A.; Rodríguez Arredondo, M.; Georg, S.; Barbosa, S. G.; Ter Heijne, A.; Hamelers, H. V. M.; Buisman, C. J. N. (Bio)electrochemical ammonia recovery: Progress and perspectives. *Applied microbiology and biotechnology* **2018**, *102*, 3865–3878.

(38) Koch, C.; Huber, K. J.; Bunk, B.; Overmann, J.; Harnisch, F. Trophic networks improve the performance of microbial anodes treating wastewater. *NPJ biofilms and microbiomes* **2019**, *5*, 27.

(39) Zinder, S. H.; Koch, M. Non-aceticlastic methanogenesis from acetate: acetate oxidation by a thermophilic syntrophic coculture. *Archive of Microbiology* **1984**, *138*, 263–272.

583 (40) Webster, T. M.; Smith, A. L.; Reddy, R. R.; Pinto, A. J.; Hayes, K. F.; Raskin, L.
584 Anaerobic microbial community response to methanogenic inhibitors 2-bromoethanesulfonate
585 and propynoic acid. *MicrobiologyOpen* **2016**, *5*, 537–550.
586 (41) Cumming, G.; Fidler, F.; Vaux, D. L. Error bars in experimental biology. *The Journal of*
587 *cell biology* **2007**, *177*, 7–11.
588 (42) Gimkiewicz, C.; Harnisch, F. Waste water derived electroactive microbial biofilms:
589 Growth, maintenance, and basic characterization. *Journal of visualized experiments : JoVE* **2013**,
590 50800.
591 (43) Kim, J. R.; Min, B.; Logan, B. E. Evaluation of procedures to acclimate a microbial fuel
592 cell for electricity production. *Applied microbiology and biotechnology* **2005**, *68*, 23–30.
593 (44) Liu, Y.; Harnisch, F.; Fricke, K.; Sietmann, R.; Schröder, U. Improvement of the anodic
594 bioelectrocatalytic activity of mixed culture biofilms by a simple consecutive electrochemical
595 selection procedure. *Biosensors & bioelectronics* **2008**, *24*, 1012–1017.
596 (45) Georg, S.; Eguren Cordoba, I. de; Sleutels, T.; Kuntke, P.; Heijne, A. T.; Buisman, C. J. N.
597 Competition of electrogens with methanogens for hydrogen in bioanodes. *Water research* **2020**,
598 *170*, 115292.
599 (46) Mansoorian, H. J.; Mahvi, A. H.; Jafari, A. J.; Khanjani, N. Evaluation of dairy industry
600 wastewater treatment and simultaneous bioelectricity generation in a catalyst-less and mediator-
601 less membrane microbial fuel cell. *Journal of Saudi Chemical Society* **2016**, *20*, 88–100.
602 (47) Liebetrau, J.; Pfeiffer, D.; Thrän, D. (H.). Collection of Measurement Methods for Biogas.
603 Methods to determine parameters for analysis purposes and parameters that describe processes in
604 the biogas sector. DBFZ. Leipzig (Series of the funding programme "Biomass energy use")
605 **2016**, *7*.
606 (48) Koch, C.; Kuchenbuch, A.; Kretzschmar, J.; Wedwitschka, H.; Liebetrau, J.; Müller, S.;
607 Harnisch, F. Coupling electric energy and biogas production in anaerobic digesters – impacts on
608 the microbiome. *RSC Adv.* **2015**, *5*, 31329–31340.
609 (49) Korth, B.; Kuchenbuch, A.; Harnisch, F. Availability of hydrogen shapes the microbial
610 abundance in biofilm anodes based on Geobacter enrichment. *ChemElectroChem* **2020,** DOI:
611 10.1002/celc.202000731.
612 (50) Hu, H.; Fan, Y.; Liu, H. Hydrogen production using single-chamber membrane-free
613 microbial electrolysis cells. *Water research* **2008**, *42*, 4172–4178.
614 (51) Martínez, E.; Sotres, A.; Arenas, C.; Blanco, D.; Martínez, O.; Gómez, X. Improving
615 Anaerobic Digestion of Sewage Sludge by Hydrogen Addition: Analysis of Microbial
616 Populations and Process Performance. *Energies* **2019**, *12*, 1228.
617 (52) Kadier, A.; Simayi, Y.; Abdeshahian, P.; Azman, N. F.; Chandrasekhar, K.; Kalil, M. S. A
618 comprehensive review of microbial electrolysis cells (MEC) reactor designs and configurations
619 for sustainable hydrogen gas production. *Alexandria Engineering Journal* **2016**, *55*, 427–443.
620 (53) Fricke, K.; Harnisch, F.; Schröder, U. On the use of cyclic voltammetry for the study of
621 anodic electron transfer in microbial fuel cells. *Energy Environ. Sci.* **2008**, *1*, 144.
622 (54) Li, T.; Zhou, Q.; Zhou, L.; Yan, Y.; Liao, C.; Wan, L.; An, J.; Li, N.; Wang, X. Acetate
623 limitation selects Geobacter from mixed inoculum and reduces polysaccharide in electroactive
624 biofilm. *Water research* **2020**, *177*, 115776.
625 (55) Koch, C.; Popiel, D.; Harnisch, F. Functional Redundancy of Microbial Anodes fed by
626 Domestic Wastewater. *CHEMELECTROCHEM* **2014**, *1*, 1923–1931.

(56) Ishii, S.'i.; Suzuki, S.; Norden-Krichmar, T. M.; Nealson, K. H.; Sekiguchi, Y.; Gorby, Y. A.; Bretschger, O. Functionally stable and phylogenetically diverse microbial enrichments from microbial fuel cells during wastewater treatment. *PloS one* **2012**, *7*, e30495.

(57) Torres, C. I.; Krajmalnik-Brown, R.; Parameswaran, P.; Marcus, A. K.; Wanger, G.; Gorby, Y. A.; Rittmann, B. E. Selecting anode-respiring bacteria based on anode potential: Phylogenetic, electrochemical, and microscopic characterization. *Environmental science & technology* **2009**, *43*, 9519–9524.

(58) Holmes, D. E.; Nevin, K. P.; Snoeyenbos-West, O. L.; Woodard, T. L.; Strickland, J. N.; Lovley, D. R. Protozoan grazing reduces the current output of microbial fuel cells. *Bioresource technology* **2015**, *193*, 8–14.

(59) Rotaru, A.-E.; Shrestha, P. M.; Liu, F.; Markovaite, B.; Chen, S.; Nevin, K. P.; Lovley, D. R. Direct interspecies electron transfer between Geobacter metallireducens and Methanosarcina barkeri. *Applied and environmental microbiology* **2014**, *80*, 4599–4605.

(60) Vrieze, J. de; Ijaz, U. Z.; Saunders, A. M.; Theuerl, S. Terminal restriction fragment length polymorphism is an "old school" reliable technique for swift microbial community screening in anaerobic digestion. *Scientific reports* **2018**, *8*, 16818.

(61) Koch, C.; Kuchenbuch, A.; Kretzschmar, J.; Wedwitschka, H.; Liebetrau, J.; Müller, S.; Harnisch, F. Coupling electric energy and biogas production in anaerobic digesters – impacts on the microbiome. *RSC Adv.* **2015**, *5*, 31329–31340.